CHAOS 28, 045101 (2018)

Simple and complex chimera states in a nonlinearly coupled oscillatory medium

Maxim Bolotov,[1] Lev Smirnov,[1,2] Grigory Osipov,[1] and Arkady Pikovsky[1,3]
[1]*Research Institute for Supercomputing, Nizhny Novgorod State University, Gagarin Av. 23, 603950 Nizhny Novgorod, Russia*
[2]*Institute of Applied Physics of the Russian Academy of Sciences, Ul'yanov Str. 46, 603950 Nizhny Novgorod, Russia*
[3]*Institute of Physics and Astronomy, University of Potsdam, Karl-Liebknecht-Str. 24/25, 14476 Potsdam-Golm, Germany*

(Received 1 November 2017; accepted 9 January 2018; published online 2 April 2018)

We consider chimera states in a one-dimensional medium of nonlinear nonlocally coupled phase oscillators. In terms of a local coarse-grained complex order parameter, the problem of finding stationary rotating nonhomogeneous solutions reduces to a third-order ordinary differential equation. This allows finding chimera-type and other inhomogeneous states as periodic orbits of this equation. Stability calculations reveal that only some of these states are stable. We demonstrate that an oscillatory instability leads to a breathing chimera, for which the synchronous domain splits into subdomains with different mean frequencies. Further development of instability leads to turbulent chimeras. *Published by AIP Publishing.* https://doi.org/10.1063/1.5011678

Oscillators can synchronize—even a weak attracting coupling can adjust their phases and frequencies. Quite surprisingly, in oscillatory media, this does not always happen even if the system is perfectly symmetric and the coupling is attractive. States with a broken symmetry, where a part of oscillators synchronize (and are ordered) and a part remains asynchronous (and are disordered), are called chimera regimes. Here, we report on interesting chimera states in a perfectly symmetric medium with nonlinear coupling. A hybrid chimera contains one fully synchronous part and another highly but not fully synchronous domain, together with asynchronous regions. A breathing chimera varies periodically in time, and its synchronous part is divided in several regions having different frequencies. In a turbulent chimera, patches of synchrony and asynchrony vary irregularly in space and time.

I. INTRODUCTION

Kuramoto and Battogtokh[1] described chimera states as a coexistence of synchrony and asynchrony in a one-dimensional oscillatory medium. The surprising feature of this finding is in breaking of the translational symmetry: although a homogeneous fully symmetric synchronous state exists and is stable, another nontrivial state may appear (from a set of initial conditions), combining synchrony and asynchrony. The level of synchrony can be characterized by a local complex order parameter. In a chimera state, this parameter is spatially inhomogeneous; moreover, in a part of the space, its absolute value is one, indicating for full local synchrony, and in another part, it is less than one, indicating for partial local synchrony.

Chimeras (see Ref. 2 for a recent review) can be found not only in an oscillatory medium,[3–7] where continuous symmetry becomes broken, but also at the interaction of several populations of oscillators,[8–11] where discrete symmetry is broken.

A significant progress in theoretical studies has been achieved by virtue of a formulation of the dynamics in terms of a local coarse-grained complex order parameter.[5,6] For this complex field, the setup becomes similar to pattern formation problems for nonlinear partial differential equations. In particular, in Ref. 12, we reduced the problem of finding stationary chimeras in the Kuramoto-Battogtokh model to that of finding periodic solutions of a system of nonlinear ordinary differential equations (ODE). For these periodic solutions, one can furthermore calculate the stability spectrum of linear perturbations, and in this way identify stable stationary chimera states.

In this paper, we apply the approach of Ref. 12 to a generalized Kuramoto-Battogtokh model suggested in Ref. 6. The difference is in a nonlinear coupling between the oscillators: the phase shift in coupling, which in the Kuramoto-Battogtokh model is assumed to be a constant, now depends on the amplitude of the acting force (see Refs. 13 and 14 for an experimental realization of such a coupling in a globally coupled population). We report below several nontrivial chimera-type states in the model with nonlinear coupling: breathing chimeras (see Ref. 15 for a short communication of this result), inhomogeneous partially synchronous states, and weakly and strongly turbulent chimeras.

II. A NONLINEARLY COUPLED OSCILLATORY MEDIUM

A. Model formulation

In this paper, we study a continuous medium of nonlocally coupled identical phase oscillators, which are distributed on a circle $0 \le x < L$, with periodic boundary conditions. In a discrete representation (used in numerical simulations below), this corresponds to a set of oscillators uniformly distributed on a ring. Each oscillator is driven by a complex coupling field $H(x, t)$ and obeys an equation

$$\dot{\varphi}(x,t) = \omega + \mathrm{Im}\big[He^{-i\varphi - i\alpha(H)}\big]\,, \tag{1}$$

where $\alpha(H) = \alpha_0 + \alpha_1|H|^2$. The problem addressed by Kuramoto and Battogtokh[1] corresponds to the case of the constant phase shift in the coupling (i.e., $\alpha_1 = 0$), the situation where the phase shift depends on the modulus of the field H was introduced in Ref. 6. The coupling field H is related to the phase oscillators via the differential equation

$$\frac{\partial^2 H}{\partial x^2} - \kappa^2 H = -\kappa^2 e^{i\varphi}\,, \tag{2}$$

solution of which can be written as an integral

$$H(x,t) = \int_0^L G(x-\tilde{x})\exp\left[i\varphi(\tilde{x},t)\right]\mathrm{d}\tilde{x}\,, \tag{3}$$

with the kernel G

$$G(y) = \frac{\kappa}{2\sinh(\kappa L/2)}\cosh[\kappa(|y| - L/2)], \quad -L/2 \le y \le L/2. \tag{4}$$

Equations (1) and (2) [or, equivalently, Eqs. (1), (3), and (4)] fully define the problem and are suitable for discretization and numerical simulations; however, they are less convenient for an analytical approach, because the phase field $\varphi(x, t)$ is generally non-continuous in x. Therefore, it is convenient to introduce a local coarse-grained (averaged over a small neighborhood $x - \delta < \tilde{x} < x + \delta$) complex order parameter

$$Z(x,t) = \frac{1}{2\delta}\int_{x-\delta}^{x+\delta} \exp\left[i\varphi(\tilde{x},t)\right]\mathrm{d}\tilde{x}\,, \tag{5}$$

which is a continuous function of the coordinate. One can achieve a significant reduction of the basic equations for the phases, if one additionally assumes, following Ott and Antonsen,[16] that the averages of the high harmonics of the phases can be expressed through this order parameter as well

$$\frac{1}{2\delta}\int_{x-\delta}^{x+\delta} \exp\left[in\varphi(\tilde{x},t)\right]\mathrm{d}\tilde{x} = [Z(x,t)]^n, \quad n \ge 1\,. \tag{6}$$

This property is invariant in time, and thus, the Ott-Antonsen manifold defined according to (6) is invariant. Therefore, the Ott-Antonsen ansatz[16] has been used in many situations and also in studies of chimeras.[2] Its validity is, however, not quite clear, as it strongly relates to the attraction properties of the Ott-Antonsen manifold (6), which are not well established. One knows that this manifold is not attractive for a population of identical oscillators in a common field.[9] In our case, we have identical oscillators in a generally inhomogeneous field $H(x, t)$. This allows assuming at least a weak attractivity of the Ott-Antonsen manifold, due to effective averaging over different driving fields in Eq. (6). With these remarks, one can consider the application of the Ott-Antonsen ansatz as a helpful, although potentially not universal reduction, suitable for a description of the long-time dynamics.[9,17]

The dynamics of the order parameter on the Ott-Antonsen manifold (6) obeys the following equation:[2,16]

$$\frac{\partial Z}{\partial t} = i\omega Z + \frac{1}{2}\left(e^{-i\alpha(H)}H - e^{i\alpha(H)}H^* Z^2\right), \tag{7}$$

while for the coupling field H we obtain the following equation from (2):

$$\frac{\partial^2 H}{\partial x^2} - \kappa^2 H = -\kappa^2 Z\,. \tag{8}$$

Before discussing the solutions of the basic model (7)–(8), we mention that there are two parameters having dimension of length: the length of the circle L and the coupling range κ^{-1}. By rescaling, we can set κ^{-1} to one, so that the only relevant parameter is L.

B. Spatially homogeneous case

The analysis of spatially homogeneous uniformly rotating states in Eqs. (7) and (8) is straightforward (in fact, the same as that of the globally coupled population with nonlinear coupling[18,19]). Substituting $Z = H = h_0 e^{i(\omega+\Omega)t}$, we obtain an equation for $|h_0|$ and Ω:

$$\begin{aligned} h_0\{|h_0|^2 \exp\left[i(\alpha_0 + \alpha_1|h_0|^2)\right] + 2i\Omega \\ - \exp\left[-i(\alpha_0 + \alpha_1|h_0|^2)\right]\} = 0\,. \end{aligned} \tag{9}$$

For all values of the parameters, there exist a fully asynchronous $h_0 = 0$ state, and a fully synchronous $|h_0| = 1$ state; for $0 < (\pi/2 - |\alpha_0|)|\alpha_1|^{-1} < 1$ there exists also a partially synchronous state with $|h_0|^2 = (\pi/2 - |\alpha_0|)|\alpha_1|^{-1}$ and $\Omega = -0.5(1 + |h_0|^2)$.

Below we restrict our attention to the domain of parameters $0 \le \alpha_0, \alpha_1 < \pi/2$. Here, the stability analysis of the homogeneous states, presented in the Appendix, gives the following results:

1. The fully asynchronous state is always unstable, because the "linear" part of coupling is attractive $0 \le \alpha_0 < \pi/2$ [see Eq. (A4)].
2. The fully synchronous state is stable, if the partially synchronous state does not exist, i.e., for $\alpha_0 + \alpha_1 < \pi/2$, and unstable otherwise [see Eq. (A5)].
3. Stability of the homogeneous partially synchronous state depends on the wavelength of the periodic in space perturbation. This state is always unstable for small wavelengths $k < k_c = \sqrt{\frac{\pi - 2\alpha_0}{\alpha_0 + \alpha_1 - \pi/2}}$, i.e., it is unstable in a long enough medium $L > L_c = 2\pi/k_c$ [see Eq. (A6)].

We see that in the presence of nonlinear coupling, a situation, where all homogeneous states are unstable, can occur. As we will show below, among stable inhomogeneous states there are also chimera states, which appear to be globally attractive.

III. STATIONARY CHIMERA STATES

A. Finding chimera profiles

Here, we discuss spatially inhomogeneous, uniformly in time rotating solutions of systems (7) and (8). We substitute

$$\begin{aligned} Z(x,t) &= z(x)\exp[i(\omega+\Omega)t], \\ H(x,t) &= h(x)\exp[i(\omega+\Omega)t], \end{aligned} \tag{10}$$

where Ω is a rotation frequency. Equation (7) reduces to an algebraic equation, from which we can express z via h

$$z(x) = -ie^{-i\alpha_0 - i\alpha_1|h|^2}\frac{\Omega+\sqrt{\Omega^2-|h|^2}}{h^*}. \tag{11}$$

Substituting this into Eq. (8), we obtain an ordinary differential equation (ODE) for the profile $h(x)$

$$h'' - h = ie^{-i\alpha_0 - i\alpha_1|h|^2}\frac{\Omega+\sqrt{\Omega^2-|h|^2}}{h^*}. \tag{12}$$

This equation is invariant to phase shifts $\arg(h)\to\arg(h)+\text{const}$, allowing for reducing to a three-dimensional real ODE. Introducing real variables (r, q) according to $h = re^{i\theta}$, $q = r^2\theta'$, we can write the resulting equations as

$$\begin{aligned} r'' &= r + \frac{q^2}{r^3} + \frac{\Omega}{r}\sin(\alpha_0+\alpha_1 r^2) - \frac{\sqrt{r^2-\Omega^2}}{r}\cos(\alpha_0+\alpha_1 r^2), \\ q' &= \Omega\cos(\alpha_0+\alpha_1 r^2) + \sqrt{r^2-\Omega^2}\sin(\alpha_0+\alpha_1 r^2), \end{aligned} \tag{13}$$

and

$$\begin{aligned} r'' &= r + \frac{q^2}{r^3} + \frac{\Omega+\sqrt{\Omega^2-r^2}}{r}\sin(\alpha_0+\alpha_1 r^2), \\ q' &= \left(\Omega+\sqrt{\Omega^2-r^2}\right)\cos(\alpha_0+\alpha_1 r^2). \end{aligned} \tag{14}$$

Equations (13) are valid in the domains where $|r| \ge |\Omega|$; here, the state is fully synchronous $|z| = 1$. Equations (14) are valid in the domains where $|r| < |\Omega|$; here, the state is asynchronous or partially synchronous $|z| < 1$.

The problem is now reduced to finding periodic (with period L) solutions of system (13),(14); such solutions exist for particular values of Ω only. It is convenient not to fix the length L, but to fix the parameter Ω, and to consider L as a function of Ω. In particular, in Figs. 1–5 below, we first fix Ω and find a stationary profile, as illustrated in panels (a) of these figures. The resulting period of this profile L, rounded to three-four significant digits, is used in the stability calculations and in the direct simulations on a periodic medium, depicted in panels (b)–(d).

Generally, one can expect many periodic solutions of system (13) and (14), because they are three-dimensional and may demonstrate sufficient complexity, including chaos. Many formal solutions are, however, excluded by the constraint $|r| < 1$. Below we focus only on the simplest periodic orbits in (13) and (14), because only they are relevant for small values of L. Systems (13) and (14) possess a symmetry $x \to -x$, $r \to r$, $q \to -q$, which allows for seeking symmetric periodic solutions, starting from point $r(0) = r_0$,

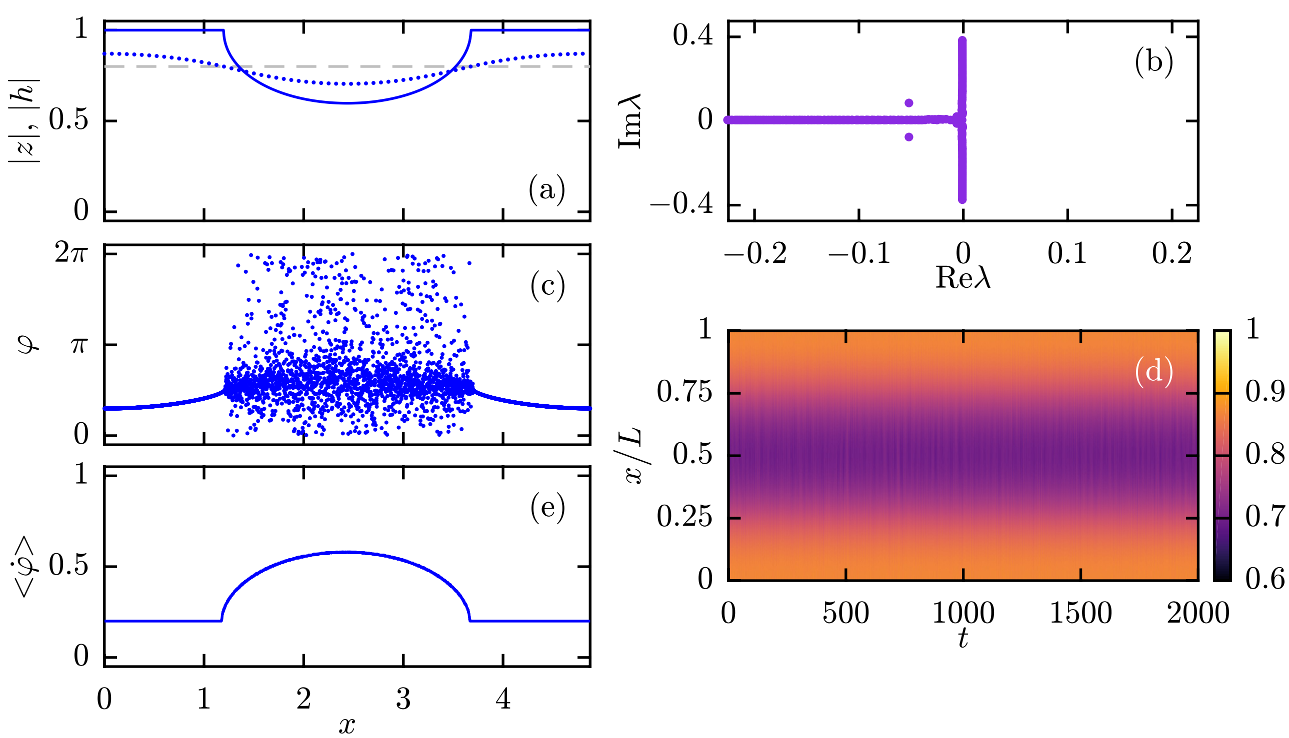

FIG. 1. Standard chimera of the Kuramoto-Battogtokh type, for $\alpha_0 = 0.3\pi$, $\alpha_1 = 0.65$, $\Omega = -0.8$, $L \approx 4.874$. Panel (a) shows profiles $|z|$ (solid line) and $|h|$ (dotted line), found with the method of Sec. III A. Here, also the level $|\Omega|$ is shown by the dashed line: the synchronous domain is that where $|H| > |\Omega|$. Panel (b) shows the spectrum of linear perturbations; here, one can clearly see complex discrete eigenvalues with negative real parts. Panels (c)–(e) show the results of direct numerical simulations of the set of $N = 4096$ oscillators. Panel (c): phases of oscillators at the end of simulations. Panel (d): spatio-temporal plot of $|H(x,t)|$. Panel (e): average frequencies of the oscillators.

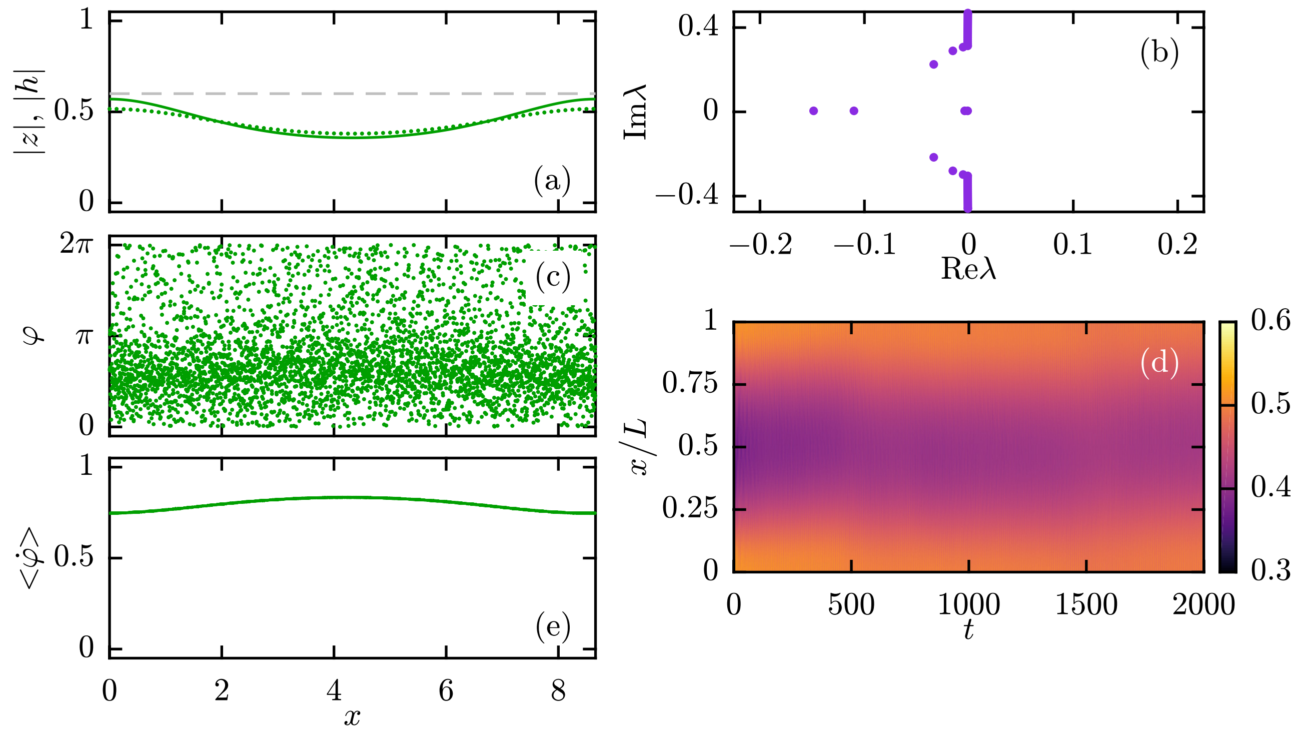

FIG. 2. Stable inhomogeneous state. Panels (a)–(e) show the same quantities as those in Fig. 1, but for $\alpha_0 = 0.4\pi$, $\alpha_1 = 1.5$, $\Omega = -0.6$, and $L \approx 8.662$.

$r'(0) = q(0) = 0$. Varying just one parameter r_0, we find periodic trajectories of (13) and (14) satisfying $r(0) = r(L)$, $r'(0) = q(0) = r'(L) = q(L) = 0$.

B. Stability of chimeras

To study the stability of the spatially inhomogeneous solutions found as described above, we transform the basic Equations (7) and (3) into the frame, rotating with frequency Ω, where solution (10) is a steady state. Linearization near this state $Z(x,t) = (z(x) + \tilde{Z}(x,t))e^{i(\omega+\Omega)t}$, $H(x,t) = (h(x) + \tilde{H}(x,t))e^{i(\omega+\Omega)t}$ yields a linear integro-differential equation

$$\frac{\partial \tilde{Z}}{\partial t} = -\left[i\Omega + e^{i\alpha} z(x) h^*(x)\right]\tilde{Z} + \frac{1}{2}(e^{-i\alpha}\tilde{H} - e^{i\alpha} z^2(x)\tilde{H}^*) - \frac{i\alpha_1}{2}(h(x)\tilde{H}^* + h^*(x)\tilde{H})\left[h(x)e^{-i\alpha} + h^*(x)z^2(x)e^{i\alpha}\right], \tag{15}$$

where $\tilde{H} = \int G(x-x')\tilde{Z}\,\mathrm{d}x'$. Introducing real variables $\tilde{Z} = \xi_1 + i\xi_2$, one can rewrite linear Eq. (15) as a system (see the Appendix for details)

$$\frac{\partial \xi}{\partial t} = (\hat{\mathbf{M}} + \hat{\mathbf{K}})\xi\,, \tag{16}$$

with a multiplicative operator $\hat{\mathbf{M}}$ and an integral operator $\hat{\mathbf{K}}$

$$\hat{\mathbf{M}} = \begin{pmatrix} \mu_1(x) & -\mu_2(x) \\ \mu_2(x) & \mu_1(x) \end{pmatrix},$$

$$\hat{\mathbf{K}}\,\xi = \begin{pmatrix} K_{11}(x) & K_{12}(x) \\ K_{21}(x) & K_{22}(x) \end{pmatrix} \int G(x-x')\,\xi(x')\,\mathrm{d}x'.$$

Expressions for μ_1, μ_2 are quite simple: for $|h| \geq |\Omega|$ $\mu_1 = -\sqrt{|h|^2 - \Omega^2}$ and $\mu_2 = 0$; for $|h| < |\Omega|$ $\mu_2 = -\sqrt{\Omega^2 - |h|^2}$ and $\mu_1 = 0$. Expressions for K_{ij} are quite lengthy and we present them in the Appendix.

General properties of the spectral problem (16) follow from the properties of the operators $\hat{\mathbf{M}}$ and $\hat{\mathbf{K}}$.[17,20] The essential spectrum is that of the multiplicative operator $\hat{\mathbf{M}}$ and has generally (if both $\mu_{1,2} \neq 0$) a T-shaped form: part of it is on the imaginary axis, and part is on the real negative axis. This essential spectrum does not contribute to instability; the latter is determined by the discrete spectrum. Numerically, it appears to be quite difficult to separate the discrete and the continuous spectral components, because due to discretization, a branch of the continuous spectrum does not exactly lie on the imaginary axis, but has nonvanishing real parts. Therefore, we apply the approach suggested in Ref. 12: if one shifts the grid on the circle $0 \leq x < L$ used in the discretization of the integral operator $\hat{\mathbf{K}}$, then the components of the continuous spectrum vary, while the components of the discrete spectrum remain stable.

IV. REGULAR CHIMERA REGIMES

In this section, we present examples of regular inhomogeneous states in the model of nonlinearly coupled oscillators. In all cases, the chimera profiles and their stability are determined as described in Sec. III. These solutions are then confirmed via direct numerical simulations.

A. Stationary chimeras

We show here three representative examples of stationary stable inhomogeneous states in Figs. 1–3.

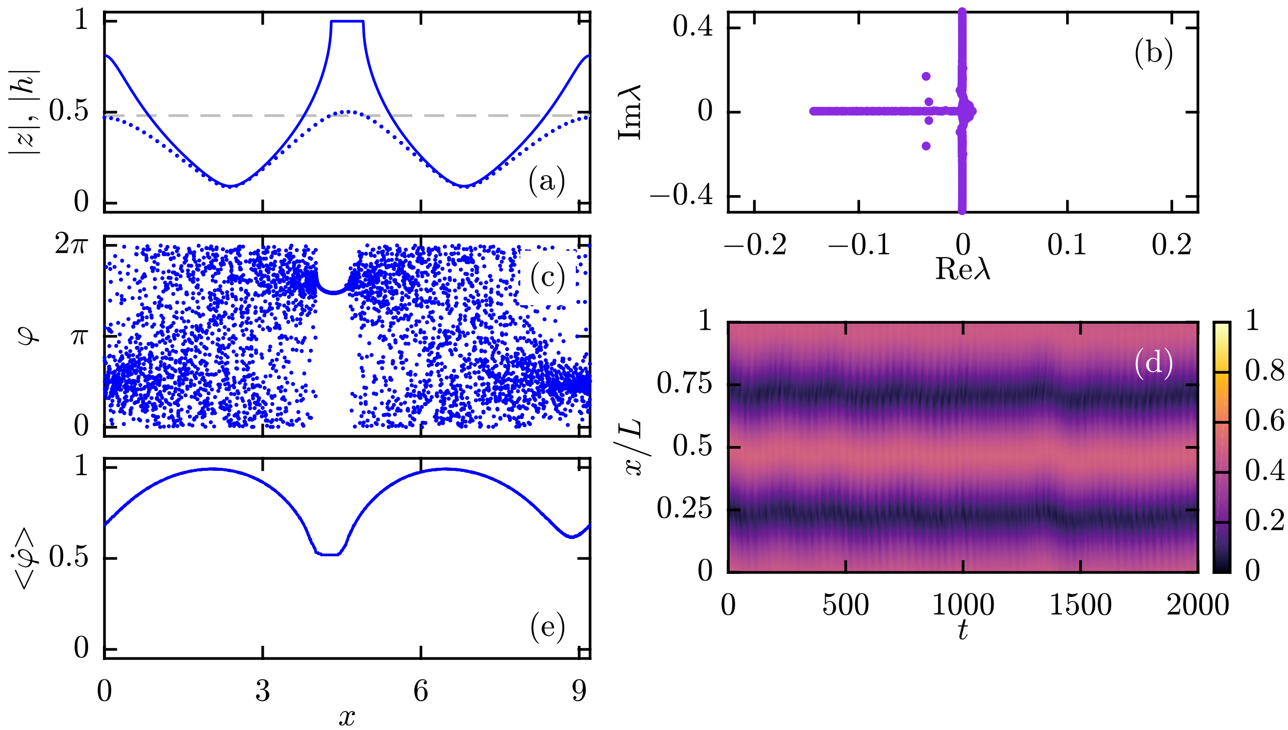

FIG. 3. Stable "hybrid" chimera state. Panels (a)–(e) show the same quantities as those in Fig. 1, but for $\alpha_0 = 0.4\pi$, $\alpha_1 = 1.5$, $\Omega = -0.48$, $L \approx 9.206$.

Figure 1 shows a standard one-cluster chimera state, as it has been first described by Kuramoto and Battogtokh.[1] Here, there is one domain where the oscillators are synchronized, and one domain with partial synchronization.

Very similar to this state is a nonhomogeneous regime illustrated in Fig. 2, where, however, there is no synchronous domain: just the level of partial synchrony varies along the space. Such states have been recently observed in Ref. 21 for a setup, where the phase shift parameter α does not depend on the modulus of the driving field $|H|$ as above, but explicitly depends on space. Noteworthy is the difference in the continuous part of the spectrum in the stability calculations

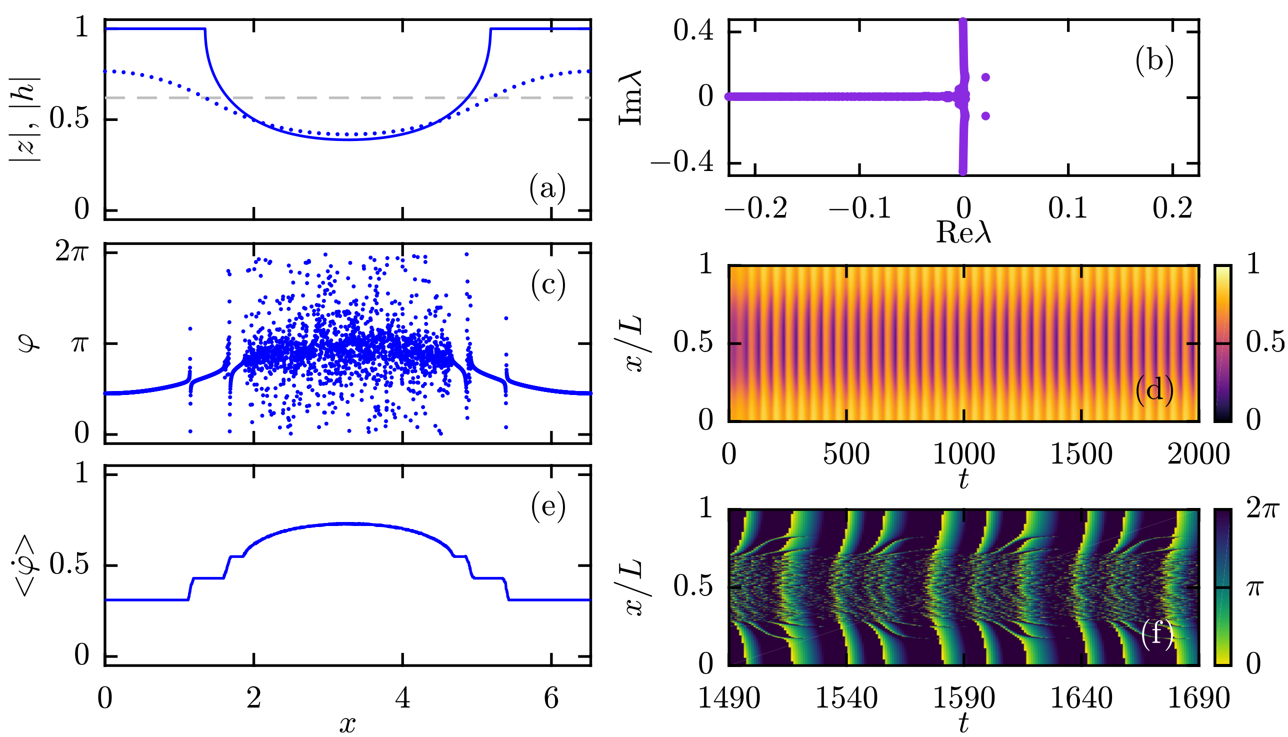

FIG. 4. Breathing chimera state. Panels (a)–(e) show the same quantities as those in Fig. 1, but for $\alpha_0 = 0.3\pi$, $\alpha_1 = 0.65$, $\Omega = -0.62$, $L \approx 6.528$. Panel (f) shows additionally the space-time plot of the phase field $\varphi(x, t)$, to illustrate the phase slips.

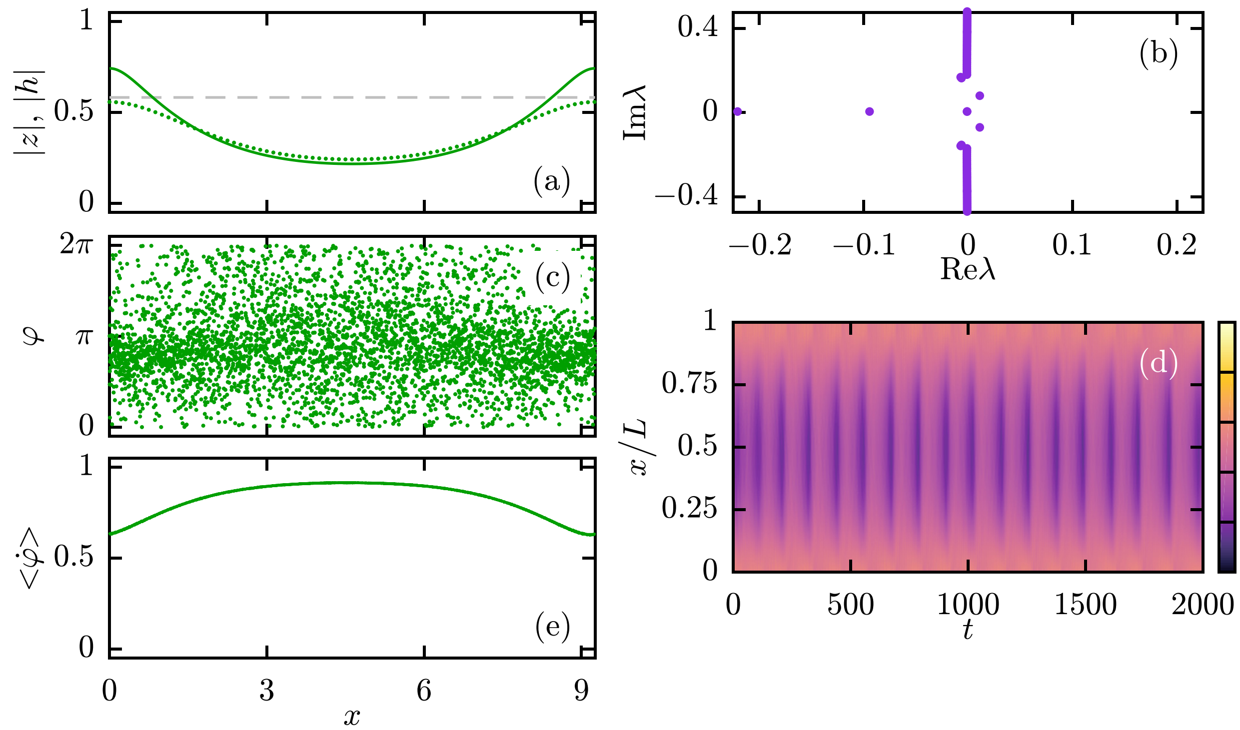

FIG. 5. Breathing inhomogeneous state. Panels (a)–(e) show the same quantities as those in Fig. 1, but for $\alpha_0 = 0.4\pi$, $\alpha_1 = 1.5$, $\Omega = -0.583$, $L \approx 9.26$.

[panel (b)]: because the synchronous domain is absent, the continuous spectrum is not T-shaped, but lies on the imaginary axis.

A stable "hybrid" state, which can be considered as a "mixture" of the two regimes of Figs. 1 and 2, is illustrated in Fig. 3. Here, a periodic in space pattern of synchrony (characterized by local values of $|z|$ and $|h|$) has two maxima. One of these maxima is completely synchronous with $|z| = 1$; another maximum is, however, only partially synchronous with $|z| < 1$. It is noteworthy that the phases in the two maxima are shifted by π.

B. Breathing chimeras

In this section, we report on breathing regimes, which appear when the states depicted in Figs. 1 and 2 become unstable. The breathing chimera is shown in Fig. 4. In panels (a) and (b), we show the stationary chimera, obtained for this value of L, and its stability: one can observe two discrete complex eigenvalues with positive real parts, indicating for oscillatory instability. Direct numerical simulations show that a stable breathing chimera appears [panel (d)]. Here, the fields $H(x,t), Z(x,t)$ vary periodically in time, but at all instants of time, there is a fully synchronous region where $|Z| = 1$.

An interesting phenomenon happens in the fully synchronous domain close to the partially synchronous one. Here, the continuous in the space phase profile is not preserved at all times: there are instants of time, at which it breaks, producing a phase slip. Deep in the synchronous domain this happens once per period of modulation, closer to the partially synchronous regime the slips happen twice during the modulation period [these slips are best seen in the space-time plot of the phases in panel (f) of Fig. 4]. Due to these slips, in the frequency profile Fig. 4(e), one observes not just one frequency plateau corresponding to the synchronous domain, but two additional subplateaus, shifted by the frequency of modulation and its second harmonics. We note that the slips could be also considered as singular violations of synchronization, e.g., the complex order parameter coarse-grained around the position of the slip vanishes at each slip event. This effect has been recently observed by Xie *et al.*[22] for two-dimensional chimera spiral regimes. There, in a domain between a disordered core and an ordered periphery, one observes detraining-entraining oscillators like in Fig. 4(c), and the corresponding steps in the mean frequency plot.

A breathing inhomogeneous state without synchronous domains appears at oscillatory instability of the stationary state of Fig. 2; it is shown in Fig. 5. This regime is very much similar to that of Fig. 4. However, because there is no synchronous domain here, there are no phase slips and the frequency profile remains smooth.

V. TURBULENT CHIMERAS

Here, we illustrate irregular states that appear in the model for relatively large values of the length L. For intermediate values of L, they may coexist with simpler states described above. In Fig. 6, we show a slightly irregular breathing chimera, which is similar to the state presented in Fig. 5. Oscillations are now aperiodic, but otherwise the spatial profile of the field $H(x, t)$ is rather regular.

A strongly turbulent state is illustrated in Fig. 7. Here, the field $H(x, t)$ is highly disordered. Nevertheless, inspection of the instantaneous phase profiles [panel (b)] reveals regions where it is locally rather smooth, indicating small domains which can be attributed to synchrony. On a long time scale,

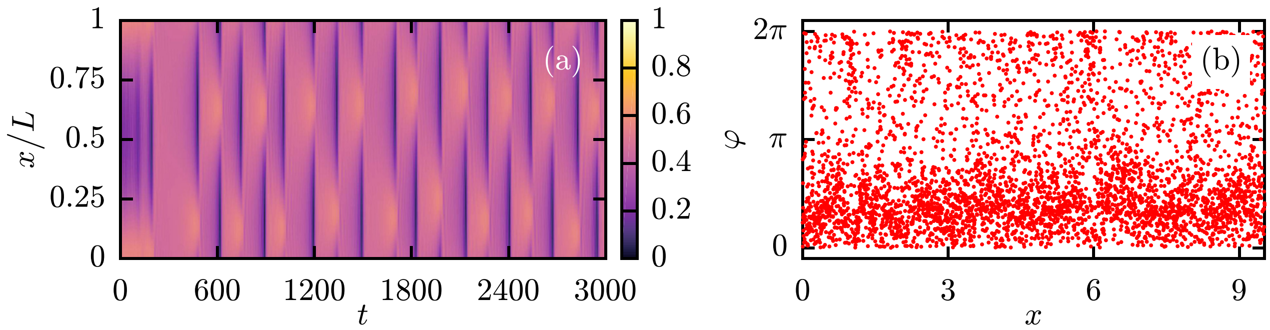

FIG. 6. Weakly irregular inhomogeneous state for $\alpha_0 = 0.4\pi$, $\alpha_1 = 1.5$, $L \approx 9.52$ (the length of the system L is slightly larger than that in Fig. 5). Panel (a): spatio-temporal dynamics of the field $|H(x,t)|$. Panel (b): a snapshot of the phases at the end of simulations.

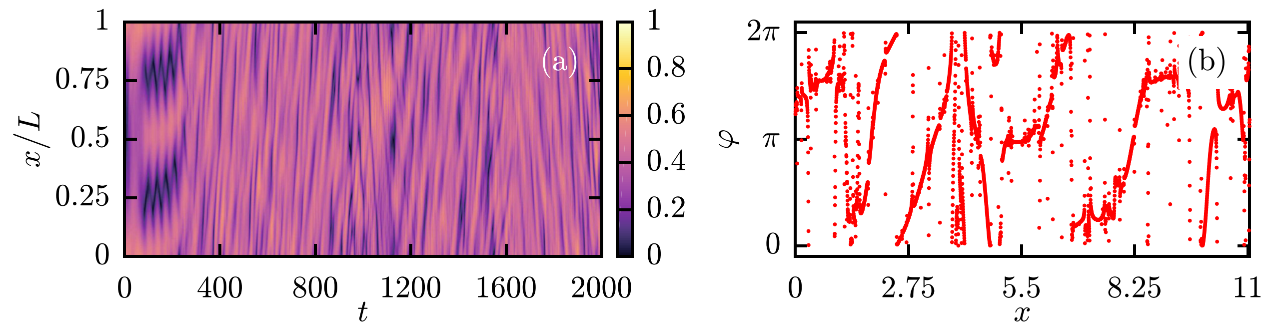

FIG. 7. Strongly irregular inhomogeneous state for $\alpha_0 = 0.4\pi$, $\alpha_1 = 1.5$, $L \approx 11.04$ (the length of the system L is larger than that in Fig. 6). Panel (a): spatio-temporal dynamics of the field $|H(x,t)|$. Panel (b): a snapshot of the phases at the end of simulations.

the dynamics of all oscillators is irregular, and the symmetry in the system is restored, although in a statistical sense. It is worth comparing these turbulent states to previously reported ones. In Ref. 6, irregular spatio-temporal solutions were reported for the same setup as in this paper, and for a chain of identical Stuart-Landau oscillators (showing that this regime is not restricted to chains of phase oscillators). Here, we support these findings by presenting Fig. 7 simulations of the phase oscillator lattice. Furthermore, we report on a weakly chaotic state in Fig. 6. In Ref. 23, a medium of non-identical oscillators was studied, i.e., at each site there was a set of oscillators with a Lorentzian distribution of frequencies. In such a system chimera states, with regions of full synchrony, are not possible. In numerical simulations of the Ott-Antonsen equations for the medium with a square kernel $G(x-y)$, Ref. 23 reports on regimes of amplitude and phase turbulence. The amplitude of the order parameter is strictly below one due to the disorder in the oscillator frequencies. In Ref. 23, no simulations of the phase oscillators are presented. In Fig. 7 one can see that in the above reported phase dynamics there are regions with rather synchronous phase profiles [seen as pieces of lines in panel (b)], what means that in the reported case the order parameter in the turbulent state can reach one.

VI. CONCLUSION

Summarizing, we have studied different chimera states in a one-dimensional medium of nonlinearly coupled phase oscillators. Our setup is almost identical to that of Kuramoto and Battogtokh, except for nonlinearity in coupling. This nonlinearity leads to novel effects (some of these effects, e.g., a turbulent state, have been reported in a short publication[6]—here, we extend this analysis by exploiting an ODE reduction for finding periodic profiles; also hybrid, breathing, and weakly chaotic chimera states were not reported in Ref. 6). First, it allows for a homogeneous partially synchronous state, which, however, becomes unstable in a long medium. In the class of stationary (uniformly rotating) spatially inhomogeneous regimes, together with the classical Kuramoto-Battogtokh chimera, we have observed an inhomogeneous partially synchronous state, and a "hybrid" chimera consisting of two domains of enhanced synchrony - one fully and another partially synchronous. Furthermore, we observed how the oscillatory instability of stationary chimeras leads to the breathing, periodically time modulated chimeras. In this regime, the synchronous domain breaks into subdomains having different oscillator frequencies. The frequency profile consists of steps, the step height is the modulation frequency. In large spatial domains, regular regimes are typically unstable and one observes either a weakly chaotic state (nonperiodically breathing chimera) or strong turbulence.

ACKNOWLEDGMENTS

Studies presented in Secs. II–IV were supported by the Russian Science Foundation (Grant No. 17–12-01534). Stability calculations in the Appendix were supported by the Russian Science Foundation (Grant No. 14–12-00811). M.B. thanks the German-Russian Interdisciplinary Science Center for support (Grant No. G-RISC M-2017a-4).

APPENDIX: STABILITY CALCULATION

Here, we present basic calculations of the stability of stationary patterns, including stability of homogeneous states. The starting point is Eq. (15)

$$\frac{\partial \tilde{Z}}{\partial t} = -\left[i\Omega + e^{i\alpha(|h|)} z(x) h^*(x)\right]\tilde{Z} + \frac{e^{-i\alpha(|h|)}}{2}\tilde{H} - \frac{e^{i\alpha(|h|)}}{2} z^2(x)\tilde{H}^* - \frac{i\alpha_1}{2}(h(x)\tilde{H}^* + h^*(x)\tilde{H})\left[h(x)e^{-i\alpha(|h|)} + h^*(x)z^2(x)e^{i\alpha(|h|)}\right], \quad \text{(A1)}$$

with $\tilde{H}(x,t) = \int G(x-\tilde{x})\tilde{Z}(\tilde{x},t)\,\mathrm{d}\tilde{x}$. We rewrite this equation as a system for two real functions $\tilde{Z}(x,t) = \xi_1(x,t) + i\xi_2(x,t)$

$$\frac{\partial \xi_1}{\partial t} = \mu_1(x)\xi_1 - \mu_2(x)\xi_2 + K_{11}(x)\int_0^L G(x-\tilde{x})\xi_1(\tilde{x},t)\,\mathrm{d}\tilde{x} + K_{12}(x)\int_0^L G(x-\tilde{x})\xi_2(\tilde{x},t)\,\mathrm{d}\tilde{x},$$
$$\frac{\partial \xi_2}{\partial t} = \mu_2(x)\xi_1 + \mu_1(x)\xi_2 + K_{21}(x)\int_0^L G(x-\tilde{x})\xi_1(\tilde{x},t)\,\mathrm{d}\tilde{x} + K_{22}(x)\int_0^L G(x-\tilde{x})\xi_2(\tilde{x},t)\,\mathrm{d}\tilde{x}\,, \quad \text{(A2)}$$

with the following notations:

$$K_{11}(x) = \frac{1}{2}[\cos\alpha - \eta_1(x)] + \alpha_1(\cos\alpha\{\chi_1(x) + 2\mathrm{Im}z(x)[\mathrm{Re}h(x)]^2\mathrm{Re}z(x)\} + \sin\alpha\{\chi_2(x) - [\mathrm{Re}h(x)]^2\}),$$
$$K_{12}(x) = \frac{1}{2}[\sin\alpha - \eta_2(x)] + \alpha_1\Big(\cos\alpha\{\chi_3(x) + [\mathrm{Im}h(x)]^2\} + \sin\alpha\Big\{-\chi_1(x) + 2\mathrm{Im}z(x)[\mathrm{Im}h(x)]^2\mathrm{Re}z(x)\Big\}\Big),$$
$$K_{21}(x) = -\frac{1}{2}[\sin\alpha + \eta_2(x)] + \alpha_1(\cos\alpha\{-\chi_2(x) - [\mathrm{Re}h(x)]^2\} + \sin\alpha\{\chi_1(x) + 2\mathrm{Im}z(x)[\mathrm{Re}h(x)]^2\mathrm{Re}z(x) - 2\mathrm{Im}h(x)\mathrm{Re}h(x)\}),$$
$$K_{22}(x) = \frac{1}{2}[\cos\alpha + \eta_1(x)] + \alpha_1(\cos\alpha\{\chi_1(x) - 2\mathrm{Im}z(x)[\mathrm{Im}h(x)]^2\mathrm{Re}z(x) - 2\mathrm{Im}h(x)\mathrm{Re}h(x)\} + \sin\alpha\{\chi_3(x) - [\mathrm{Im}h(x)]^2\}),$$

$$\mu_1(x) = \begin{cases} -\sqrt{|h(x)|^2 - \Omega^2}, & |h(x)| \ge \Omega, \\ 0, & |h(x)| < \Omega, \end{cases}$$
$$\mu_2(x) = \begin{cases} 0, & |h(x)| \ge \Omega, \\ -\sqrt{\Omega^2 - |h(x)|^2}, & |h(x)| < \Omega, \end{cases}$$

$$\eta_1(x) = [\mathrm{Re}z(x)]^2\cos\alpha - [\mathrm{Im}z(x)]^2\cos\alpha - 2\mathrm{Re}z(x)\mathrm{Im}z(x)\sin\alpha,$$
$$\eta_2(x) = [\mathrm{Re}z(x)]^2\sin\alpha - [\mathrm{Im}z(x)]^2\sin\alpha + 2\mathrm{Re}z(x)\mathrm{Im}z(x)\cos\alpha,$$

$$\chi_1(x) = \mathrm{Im}h(x)\mathrm{Re}h(x) + \mathrm{Im}h(x)[\mathrm{Im}z(x)]^2\mathrm{Re}h(x) - \mathrm{Im}h(x)\mathrm{Re}h(x)[\mathrm{Re}z(x)]^2,$$
$$\chi_2(x) = -[\mathrm{Im}z(x)]^2[\mathrm{Re}h(x)]^2 + 2\mathrm{Im}h(x)\mathrm{Im}z(x)\mathrm{Re}h(x)\mathrm{Re}z(x) + [\mathrm{Re}z(x)]^2[\mathrm{Re}h(x)]^2,$$
$$\chi_3(x) = [\mathrm{Im}h(x)]^2[\mathrm{Im}z(x)]^2 + 2\mathrm{Im}h(x)\mathrm{Im}z(x)\mathrm{Re}h(x)\mathrm{Re}z(x) - [\mathrm{Im}h(x)]^2[\mathrm{Re}z(x)]^2.$$

Equation (A2) is Eq. (16) in the main text.

Next we discuss, using Eq. (A2), the stability of spatially homogeneous states. In this case, the solutions are plane waves $\boldsymbol{\xi}(x,t) = \boldsymbol{A}e^{-ikx+\lambda t}$, $\boldsymbol{A} = (A_1, A_2)^T$, and the eigenvalue equation for λ is

$$\lambda\boldsymbol{A} = \left[\hat{\mathbf{M}}_0 + I(k)\hat{\mathbf{K}}_0\right]\boldsymbol{A}\,, \quad \text{(A3)}$$

with $I(k) = \int_{-L/2}^{L/2} G(x)e^{ikx}\,\mathrm{d}x = \frac{1}{1+k^2}$. Operators $\hat{\mathbf{M}}_0, \hat{\mathbf{K}}_0$ are defined according to Eq. (16) and expressions above, subindex 0 means that the corresponding steady solutions of Eq. (9), z_0, and h_0 are inserted.

For the fully asynchronous state, we have $Z_{as} = z_0 = h_0 = 0$, $\alpha = \alpha_0$. Here, the eigenvalues are

$$\lambda_{1,2} = \frac{1}{2}(1+k^2)^{-1}\cos(\alpha_0) \pm i\sqrt{\left|\frac{1}{2}\sin(\alpha_0) + \Omega\right|}. \quad \text{(A4)}$$

For the fully synchronous state $Z_s = e^{i(\omega+\Omega_s)t}$ with $\Omega_s = -\sin(\alpha_0+\alpha_1)$, $z_0 = 1$, $h_0 = 1$, $\alpha = \alpha_0 + \alpha_1$. The eigenvalue problem can be solved as

$$\begin{aligned}\lambda_1 &= -\cos(\alpha_0+\alpha_1), \\ \lambda_2 &= -\cos(\alpha_0+\alpha_1)[1-(1+k^2)^{-1}]\,.\end{aligned} \quad \text{(A5)}$$

For a partially synchronous state, we have $Z_{ps} = r_{ps}e^{i(\omega+\Omega_{ps})t}$, where $r_{ps} = \sqrt{\frac{\pi/2-\alpha_0}{\alpha_1}}$, $z_0 = r_{ps}$, $h_0 = r_{ps}$, $\alpha = \alpha_0 + \alpha_1 r_{ps}^2$, $\Omega_{ps} = -(1+r_{ps}^2)/2$. Here, the solution of the eigenvalue problem reads

$$\lambda_{1,2} = \frac{(\pi/2-\alpha_0)(\pi/2-\alpha_0-\alpha_1)}{2\alpha_1(1+k^2)} \pm \frac{1}{2}\left[\frac{(\pi/2-\alpha_0)^2(\pi/2-\alpha_0-\alpha_1)^2}{\alpha_1^2(1+k^2)^2} - \frac{\alpha_1^2-\alpha_0^2-(\pi/2)^2+\pi\alpha_0}{\alpha_1^2}\frac{k^4}{(1+k^2)^2} + \frac{(\pi/2-\alpha_0)(\alpha_1+\alpha_0-\pi/2)}{\alpha_1^2}\frac{2k^2}{(1+k^2)}\right]^{1/2}. \quad \text{(A6)}$$

The condition $\lambda_1 = 0$ yields the critical wave number $k_c^2 = \frac{\pi-2\alpha_0}{\alpha_1-\pi/2+\alpha_0}$.

[1]Y. Kuramoto and D. Battogtokh, "Coexistence of coherence and incoherence in nonlocally coupled phase oscillators," Nonlinear Phenom. Complex Syst. **5**, 380–385 (2002).
[2]M. J. Panaggio and D. M. Abrams, "Chimera states: Coexistence of coherence and incoherence in networks of coupled oscillators," Nonlinearity **28**, R67–R87 (2015).
[3]D. M. Abrams and S. H. Strogatz, "Chimera states for coupled oscillators," Phys. Rev. Lett. **93**, 174102 (2004).
[4]S.-I. Shima and Y. Kuramoto, "Rotating spiral waves with phase-randomized core in nonlocally coupled oscillators," Phys. Rev. E **69**, 036213 (2004).
[5]C. R. Laing, "The dynamics of chimera states in heterogeneous Kuramoto networks," Phys. D: Nonlinear Phenom. **238**, 1569–1588 (2009).
[6]G. Bordyugov, A. Pikovsky, and M. Rosenblum, "Self-emerging and turbulent chimeras in oscillator chains," Phys. Rev. E **82**, 035205 (2010).
[7]Y. L. Maistrenko, A. Vasylenko, O. Sudakov, R. Levchenko, and V. L. Maistrenko, "Cascades of multiheaded chimera states for coupled phase oscillators," Int. J. Bifurcation Chaos **24**, 1440014 (2014).
[8]D. M. Abrams, R. Mirollo, S. H. Strogatz, and D. A. Wiley, "Solvable model for chimera states of coupled oscillators," Phys. Rev. Lett. **101**, 084103 (2008).
[9]A. Pikovsky and M. Rosenblum, "Partially integrable dynamics of hierarchical populations of coupled oscillators," Phys. Rev. Lett. **101**, 264103 (2008).
[10]M. R. Tinsley, S. Nkomo, and K. Showalter, "Chimera and phase-cluster states in populations of coupled chemical oscillators," Nat. Phys. **8**, 662–665 (2012).
[11]E. A. Martens, S. Thutupalli, A. Fourrière, and O. Hallatschek, "Chimera states in mechanical oscillator networks," Proc, Natl. Acad. Sci. **110**, 10563–10567 (2013).
[12]L. Smirnov, G. Osipov, and A. Pikovsky, "Chimera patterns in the Kuramoto-Battogtokh model," J. Phys. A: Math. Theor. **50**, 08LT01 (2017).
[13]A. A. Temirbayev, Z. Z. Zhanabaev, S. B. Tarasov, V. I. Ponomarenko, and M. Rosenblum, "Experiments on oscillator ensembles with global nonlinear coupling," Phys. Rev. E **85**, 015204 (2012).
[14]A. A. Temirbayev, Y. D. Nalibayev, Z. Z. Zhanabaev, V. I. Ponomarenko, and M. Rosenblum, "Autonomous and forced dynamics of oscillator ensembles with global nonlinear coupling: An experimental study," Phys. Rev. E **87**, 062917 (2013).
[15]M. I. Bolotov, L. A. Smirnov, G. V. Osipov, and A. Pikovsky, "Breather chimera states in a system of phase oscillators," JETP Lett. **106**, 393 (2017).
[16]E. Ott and T. M. Antonsen, "Low dimensional behavior of large systems of globally coupled oscillators," CHAOS **18**, 037113 (2008).
[17]M. Wolfrum, O. E. Omel'chenko, S. Yanchuk, and Y. L. Maistrenko, "Spectral properties of chimera states," CHAOS **21**, 013112 (2011).
[18]M. Rosenblum and A. Pikovsky, "Self-organized quasiperiodicity in oscillator ensembles with global nonlinear coupling," Phys. Rev. Lett. **98**, 064101 (2007).
[19]A. Pikovsky and M. Rosenblum, "Self-organized partially synchronous dynamics in populations of nonlinearly coupled oscillators," Phys. D **238**(1), 27–37 (2009).
[20]O. E. Omel'chenko, "Coherence-incoherence patterns in a ring of nonlocally coupled phase oscillators," Nonlinearity **26**, 2469 (2013).
[21]C.-U. Choe, R.-S. Kim, and J.-S. Ri, "Chimera and modulated drift states in a ring of nonlocally coupled oscillators with heterogeneous phase lags," Phys. Rev. E **96**, 032224 (2017).
[22]J. Xie, E. Knobloch, and H.-C. Kao, "Twisted chimera states and multicore spiral chimera states on a two-dimensional torus," Phys. Rev. E **92**, 042921 (2015).
[23]M. Wolfrum, S. V. Gurevich, and O. E. Omelchenko, "Turbulence in the Ott - Antonsen equation for arrays of coupled phase oscillators," Nonlinearity **29**, 257 (2016).